Waste Disposal & Sustainable Energy (2022) 4:259–269
https://doi.org/10.1007/s42768-022-00108-0

ARTICLE

Novel development of VO_x–CeO_x–WO_x/TiO_2 catalyst for low-temperature catalytic oxidation of chloroaromatic organics

Yunfeng Ma[1] · Jianwen Lai[1] · Jiayao Wu[1] · Xiaoqing Lin[1] · Hong Yu[1] · Hao Zhang[1] · Angjian Wu[1] · Jisheng Long[2] · Xiaodong Li[1]

Received: 15 July 2022 / Revised: 11 August 2022 / Accepted: 16 August 2022 / Published online: 4 October 2022

Abstract

A novel selective catalytic reduction (SCR) catalyst with high catalytic activity on chloroaromatic organics at lower temperatures (160–180 ℃) is critical for municipal solid waste incineration (MSWI) plants. This study prepares a series of honeycomb-type VO_x/TiO_2 catalysts and finally develops a new low-temperature catalyst with high catalytic activity in eliminating chloroaromatic organics. Based on the conversion efficiency (CE) of 1,2-dichlorobenzene (1,2-DCB) and CO_2 selectivity, the optimal VO_x content of 4.06% (in weight) in VO_x/TiO_2 catalyst is first confirmed. By modifying CeO_x and WO_x, a novel honeycomb-type catalyst of VO_x–CeO_x–WO_x/TiO_2 achieves the highest CE (93.1%–93.6%) and CO_2 selectivity (40.9%–60.7%) at 150–200 ℃. It was found that the CeO_x and WO_x can improve the catalytic activity by enriching the surface content of V and O, increasing the proportion of V^{5+} and O_{surf}, enlarging the supply source of reactive oxygen species and their storage capacity, and accelerating the redox cycle of VO_x, CeO_x, WO_x, and reactive oxygen species. This study can guide the development of monolithic low-temperature catalysts with high catalytic activity in eliminating chloroaromatic organics in MSWI flue gas.

Keywords VO_x/TiO_2 catalysts · Honeycomb catalysts · Catalytic activity · 1,2-dichlorobenzene · Modification of CeO_x and WO_x

Introduction

Incineration has become the major disposal route (62.1%) of municipal solid waste (MSW) in China [1]. However, the emission of chloroaromatic organics is always the focused problem, especially the extremely toxic polychlorinated-ρ-dibenzodioxins and dibenzofurans (PCDD/Fs) and their essential precursor of chlorobenzene with higher concentration (800–46,600 ng/Nm^3) [2]. Significant efforts have been made to control their emission, of which, the adsorption method (active carbon injection coupled with fabric filter) is the widespread and efficient technology, but it only achieves contaminants transfer without amount reduction and needs further treatment. In comparison, the catalytic oxidation has technical advantages, which can completely mineralize chloroaromatic organics into CO_2, H_2O, and HCl as well as control the NO_x emission [2–5].

Several DeNO$_x$ selective catalytic reduction (SCR) systems that applied TiO_2-supported oxides of vanadium (VO_x/TiO_2) catalysts have been proven the positive catalytic effect on PCDD/F removal [6–8]. Our previous study reported the sulfur-resistance advantages of TiO_2, and VO_x was evaluated as the best single transition metal oxide for eliminating PCDD/Fs over the TiO_2 support [9]. However, to improve the catalytic activity of VO_x/TiO_2 and overcome the multiple poisoning effect from the complex flue gas from MSW incineration (MSWI), a second catalytic component is usually introduced into VO_x/TiO_2 catalysts, such as WO_x, MoO_x, MnO_x, and CeO_x [3, 10, 11]. Wherein, the V_2O_5–WO_3/TiO_2 catalyst is widely used for DeNO*x*, and it shows effective synergistic elimination of both PCDD/

✉ Xiaoqing Lin
linxiaoqing@zju.edu.cn

✉ Jisheng Long
long@shjec.cn

[1] State Key Laboratory for Clean Energy Utilization, Institute for Thermal Power Engineering, Zhejiang University, Hangzhou 310027, China

[2] Shanghai SUS ENVIRONMENT Co., LTD, Shanghai 201703, China

Fs and NO_x with high removal efficiency (RE) of 99% and 90%, respectively, at 230 °C [12]. Our previous studies also investigated the synergistic removal effect on PCDD/Fs and NO_x by the actual SCR equipped with V_2O_5–Mo_2O_3/TiO_2 in the MSWI plant, which has a high RE on NO_x (82.3%) but a low RE on PCDD/Fs (27.6%) at 180 °C [13]. Thus, the operating temperature of SCR in the MSWI plant is usually higher than 200 °C to ensure the effective removal of NO_x, which requires an auxiliary device and additional energy to reheat the fabric filter exhaust (about 160 °C) [14]. Herein, it is particularly critical to develop a new catalyst with a better elimination effect in the low-temperature window (150–200 °C).

To achieve these goals, only increasing the content of VO_x should not be a good option, as a high VO_x content will cause high oxidation of SO_2 to SO_3 and lead to serious S-poisoning problems [10, 11]. Based on the optimum VO_x content, introducing a second or third active component or promoter could be a practical proposal. CeO_2 is a feasible selection due to the unique and flexible redox couple Ce^{4+}/Ce^{3+}, which can promise the catalysts with great oxygen storage/release capacity under oxidizing or reducing conditions [7, 15]. Our previous study compared the promotion effect of WO_x, MoO_x, MnO_x, and CeO_x and identified CeO_x as the best one, followed by MnO_x, WO_x, and MoO_x [9]. The VO_x(5%)–CeO_x(5%)/TiO_2 shows a high PCDD/F degradation efficiency of 92.5% at 200 ℃ [9]. The introduction of WO_x or MoO_x can improve the catalytic activity and stability of VO_x/TiO_2 by suppressing sintering and retarding the phase transformation from anatase to rutile-TiO_2 [3, 10, 11]. However, previous studies have mainly been conducted under lab conditions over powder catalysts, which is not convenient for field application due to their ignorable disadvantages, such as a lack of no macroscopic geometric structure and mechanical strength, large differential pressure of the catalyst bed, and inconvenient cleaning and replacing, etc. [16]. Monolithic catalysts can overcome such disadvantages and are normally shaped as honeycombs [3, 11]. Metallic monoliths have additional advantages such as good resistance to thermal shock and uniform temperature distribution, which can be better adapted to the actual SCR system [17]. Therefore, it is urgent to develop honeycomb-type catalysts with high RE on chloroaromatic organics in a low operating temperature window (150–200 °C).

In this study, a series of honeycomb-type VO_x/TiO_2, VO_x–CeO_x/TiO_2, VO_x–WO_3/TiO_2, and VO_x–CeO_x–WO_x/TiO_2 catalysts are prepared by the extruding method, and their activity for 1,2-dichlorobenzene (1,2-DCB) catalytic oxidation is experimentally evaluated at low temperatures (150–200 °C). Finally, a newly developed VO_x–CeO_x–WO_x/TiO_2 catalyst shows excellent catalytic activity on 1,2-DCB conversion. This study tries to guide engineering technicians in rationally designing catalysts for the efficient destruction of chloroaromatic organics at a low temperatures.

Materials and methods

Catalyst preparation

The prepared TiO_2-supported Vanadium oxides (VO_x/TiO_2) catalysts are honeycomb-type monolithic catalysts and are synthesized by the extruding method. It includes eight steps, i.e., (1) pretreatment of powder material, (2) mixing of dried powders, (3) stirring of wet powders, (4) pre-squeezing of wet material, (5) settling of the squeezed material, (6) extruding as honeycomb type, (7) drying of the honeycomb-type catalyst, and (8) calcining of dried catalyst. As shown in Table 1, the catalysts consist of carrier (TiO_2), active components (VO_x, CeO_x, and WO_x), and some other residues of SiO_2, Na, Ca, and S. The commercial titanium dioxide and the first batch of shaping additives (including carboxymethyl cellulose, polyethylene oxide, and fiber) are added to the machine for stirring. The VO_x precursor (NH_4VO_3), CeO_x precursor ($Ce(NO_3)_3{\cdot}6H_2O$), and WO_x precursor ($(NH_4)_6H_2W_{12}O_{40}{\cdot}H_2O$) are dissolved in deionized water, and then introduced into the obtained mixture. Next, other shaping additives (including stearic acid and lactic acid) and deionized water are gradually added to the stirring machine in steps. Then, the wet catalyst mixture is obtained for further extruding into a honeycomb-like structure. To obtain the final version of honeycomb-type catalysts, the wet catalysts

Table 1 The major components and contents of catalysts (% in weight)

Samples	Code	V_2O_5	CeO_2	WO_3	TiO_2	SiO_2	Na	Ca	S
VO_x/TiO_2	V(1.5)/Ti	1.50	–	–	90.70	2.79	1.01	0.70	0.55
	V(2.5)/Ti	2.56	–	–	90.58	2.16	0.81	0.54	0.38
	V(4.0)/Ti	4.06	–	–	87.59	3.73	1.17	0.81	0.55
	V(5.5)/Ti	5.74	–	–	88.06	2.35	0.78	0.59	0.38
	V(8.0)/Ti	8.07	–	–	87.34	1.49	0.81	0.38	0.30
VO_x–CeO_x/TiO_2	V–Ce/Ti	3.96	2.75	–	83.54	5.03	0.75	1.04	0.57
VO_x–WO_x/TiO_2	V–W/Ti	3.74	–	2.65	82.86	5.60	0.78	1.19	0.49
VO_x–CeO_x–WO_x/TiO_2	V–Ce–W/Ti	3.97	3.04	2.91	82.01	3.48	0.71	0.79	0.78

are further dried and calcined under programmed temperature procedures for approximately 24 h in an air atmosphere. The Eq. 1 illustrates the drying temperature program, which will reduce the moisture from 24.5% to 5.0% (in weight). On the one hand, the multi-stage temperature can effectively promote additive stabilization and catalyst shaping; on the other hand, it can prevent wall cracking due to the rapid loss of moisture and prepare well for the following calcining procedures. The calcining program (Eq. 2) is also conducted under multi-stage temperature designed for different purposes, i.e., moisture removal (100 °C), decomposition of organic additives (250 °C), precursor decomposition of active components (350 °C), and valance optimum of V, Ce, W, and O, as well as residue removal (450 °C).

Programmed temperature procedures for catalyst drying:

$$\begin{aligned}&\text{Room temperature} \xrightarrow{10^{\circ}\text{C/min}} 65^{\circ}\text{C} \xrightarrow{60\,\text{min}} 65^{\circ}\text{C}\\ &\xrightarrow{5^{\circ}\text{C/min}} 80^{\circ}\text{C} \xrightarrow{60\ \text{min}} 80^{\circ}\text{C} \xrightarrow{5^{\circ}\text{C/min}} 105^{\circ}\text{C} \xrightarrow{60\,\text{min}}\\ &105^{\circ}\text{C} \xrightarrow{\text{Free cooling}} \text{Room temperature}\end{aligned} \quad (1)$$

Programmed temperature procedures for catalyst calcining:

$$\begin{aligned}&\text{Room temperature} \xrightarrow{15\,^{\circ}\text{C/min}} 100\,^{\circ}\text{C} \xrightarrow{120\ \text{min}} 100\\ &,^{\circ}\,\text{C} \xrightarrow{7.5\,^{\circ}\text{C/min}} 250\,^{\circ}\text{C} \xrightarrow{150\ \text{min}} 250\,^{\circ}\text{C}\\ &\xrightarrow{5\,^{\circ}\text{C/min}} 350\,^{\circ}\text{C} \xrightarrow{150\ \text{min}} 350\,^{\circ}\text{C} \xrightarrow{5\,^{\circ}\text{C/min}}\\ &450\,^{\circ}\text{C} \xrightarrow{720\ \text{min}} 450\,^{\circ}\text{C} \xrightarrow{\text{Free cooling}} \text{Room temperature}\end{aligned} \quad (2)$$

Catalytic activity tests

In this study, the 1,2-DCB, a representative chloroaromatic organic and modeling target of PCDD/Fs, is used to evaluate the catalytic activities of the series of VO_x/TiO_2 catalysts based on laboratory instruments (Fig. 1). As shown in Fig. 1, the initial 1,2-DCB is generated by the bubbling method. The prepared catalysts are loaded in a vertical quartz tube reactor (28 cm length×18 mm inner diameter), which is installed in an electric furnace. The real-time reaction temperature is detected by a K-type thermocouple close to the catalyst bed and is controlled by a regulator. The concentration of 1,2-DCB was monitored online (detection frequency: once every 4 min) by a gas chromatograph (GC, TRACE 1300, ThermoFisher Scientific, Waltham, MA, USA) equipped with a DB-5 column (30 m length×0.25 mm inner diameter×0.25 μm film) and a flame ionization detector (FID). In addition, this GC workshop is usually calibrated by standard gas of 1,2-DCB every 3 months to ensure detection accuracy. The CO_2 is detected by an online instrument of GYU-M500 (0–1000×10^{-6}) equipped with non-dispersive infrared (NDIR) sensors (model: GYU-W150; detection accuracy: 0.1×10^{-6}), which is calibrated by the standard gas CO_2 every 2 months.

In this study, the reaction temperature ranged from 150 °C to 200 °C (low-temperature windows) with an interval of 10 °C. The average initial concentration of 1,2-DCB is approximately 99.4×10^{-6}±1.3×10^{-6}. To obtain an accurate conversion efficiency (CE) of 1,2-DCB, at least 8 consecutive and stable concentration values of 1,2-DCB in off-gas were collected at each reaction temperature. To reduce the influence on the reaction equilibrium, the heating rate was set as low as 1.0 °C/min. The reaction flow was 150 mL/min, controlled by the mass flowmeter. 1.5 mL of each catalyst was prepared into a cordierite honeycomb module with a size of 13.0 mm×13.0 mm×21.7 mm. The channels are of square cross-section 5.0 mm×5.0 mm with walls of 1.0 mm thickness. That is, each experiment is conducted under the gas hourly space velocity (GHSV) of 6000 per h.

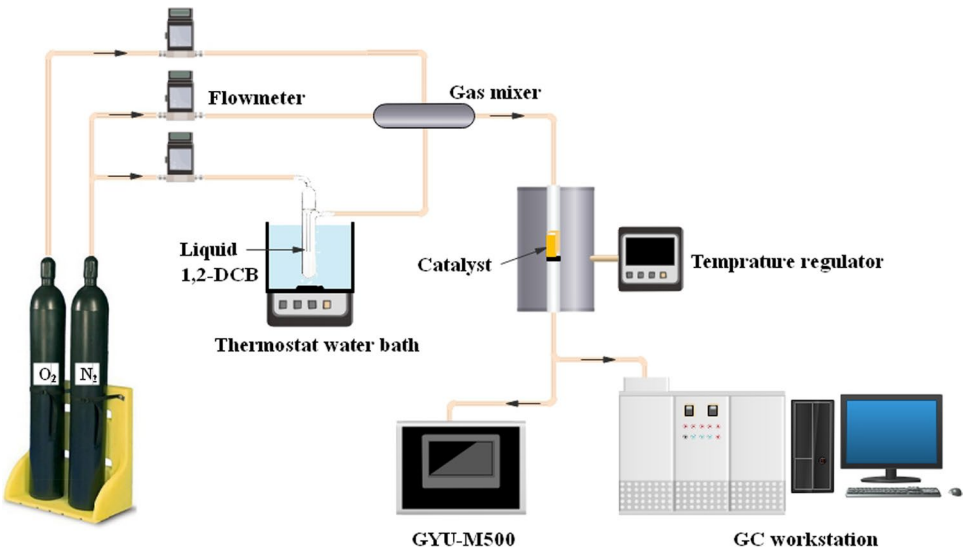

Fig. 1 The evaluation system of catalytic activity on 1,2-DCB (1,2-dichlorobenzene). *GC* gas chromatograph

The CE of 1,2-DCB and the selectivity of CO_2 are defined according to Eqs. 3 and 4 [18]. The CO_2 selectivity represents the conversion rate of the eliminated part of 1,2-DCB in this study, i.e., the complete oxidative capacity of catalysts.

$$1,2-\mathrm{DCB\ conversion}\,(\%) = \frac{[1,2-\mathrm{DCB}]_{\mathrm{in}} - [1,2-\mathrm{DCB}]_{\mathrm{out}}}{[1,2-\mathrm{DCB}]_{\mathrm{in}}} \times 100\% \quad (3)$$

$$\mathrm{CO_2\ selectivity}\,(\%) = \frac{[\mathrm{CO_2}]_{\mathrm{out}}}{6 \times ([1,2-\mathrm{DCB}]_{\mathrm{in}} - [1,2-\mathrm{DCB}]_{\mathrm{out}})} \times 100\% \quad (4)$$

where the "in" and "out" subscripts are indicative of the inlet and outlet concentrations of 1,2-DCB and CO_2 at a steady-state, respectively.

Catalyst characterization

To better reveal the catalytic activity and promotion reasons of the series catalysts, the chemical compositions of each catalyst were detected by a wavelength-dispersive X-ray fluorescence (XRF) spectrometer (ADVANT'X 4200, Thermo Fisher Scientific, Waltham, MA, USA) according to the GB/T 31590-2015 [19]. The X-rays were generated with an Rh anode, and calibration with a series of metal standards and UniQuant software is used for quantitative analysis. The specific surface area and average pore size were detected by the Brunner-Emmet-Teller (BET) measurements (TRISTAR 3020, Micromeritics Instrument Corporation, Norcross, GA, USA). The total pore volume was calculated by the method of Barrett-Joyner-Halenda (BJH). X-ray photoelectron spectroscopy (XPS, ESCALAB 250Xi, Thermo Fisher Scientific Inc., Waltham, MA, USA) with Al Kα X-rays was applied to determine the valence state of the surface elements.

Results and discussion

Catalyst characterizations

Chemical compositions

In this study, novel catalyst development can be divided into two stages, i.e., finding the optimal VO_x content for the VO_x/TiO_2 catalyst, and introducing second (Ce) or third (W) active components or promoters into the optimal VO_x/TiO_2 catalyst. The chemical compositions of the series catalysts are summarized in Table 1. The content grades of VO_x are distributed as 1.50%, 2.56%, 4.06%, 5.74%, and 8.07% (in weight). Finocchio et al. summarized and reported that the optimal VO_x content in VO_x-WO_x/TiO_2 ranged from 3% to 4% (in weight), and the highest content should not be higher than 7%–8% (in weight), based on multiple factors, such as catalytic activity, and manufacturing cost [20]. Wang et al. reported that 3%–5% (in weight) V_2O_5 catalysts are the best fit for chlorobenzene oxidation [4]. To increase the oxygen storage/release capacity of VO_x/TiO_2 as well as widen the reaction temperature [3, 15, 21], CeO_x (approximately 3% (in weight)) is introduced into the catalyst formulation (VO_x–CeO_x/TiO_2 and VO_x–CeO_x–WO_x/TiO_2). To inhibit the initial sintering of TiO_2 and improve the SO_2 resistance [10, 11, 22], WO_x (approximately 3% (in weight)) is also introduced (VO_x–WO_x/TiO_2 and VO_x–CeO_x–WO_x/TiO_2). By increasing the VO_x content and introducing CeO_x and WO_x, the content of TiO_2 is generally decreased from 90.70% to 82.01% (in weight) (Table 1). Some other components (Si, Na, Ca, and S) are also detected, which could be either introduced from the commercial titanium dioxide (not pure TiO_2) or from the shaping additives ("Catalyst preparation"). Their irregular contents can be attributted to the catalyst preparation process and the limitations of the XRF method.

Porous structure

The first step and basic guarantee of catalytic reaction processes is surface adsorption of 1,2-DCB, including physisorption and chemisorption, and the former is closely related to the specific surface area and pore structure [11]. As shown in Table 2, the BET parameters of series catalysts are summarized. Compared with the original TiO_2, the loading of active components (VO_x, CeO_x, and WO_x) significantly decreases the surface area (i.e., from 90.2 m^2/g to 31.5–67.8 m^2/g) and mesopore area (i.e., from 81.1 m^2/g to 26.4–60.4 m^2/g), but the loading process does not change the domination of mesopore area, which corresponds to previous studies [4, 23]. The decrease in BET parameters could be attributed to the following aspects: (1) the loading of active components blocks the voids and surface of TiO_2, and (2) the calcination induces the TiO_2 agglomeration.

By increasing the VO_x content, the surface area first increases from 49.7 m^2/g (V(1.5)/Ti) to 58.9 m^2/g (V(5.5)/Ti), and then distinctly decreases to 31.5 m^2/g (V(8.0)/Ti). A similar changing trend is also observed in the mesopore area. However, the ratio of mesopore area to surface area continuously increases with increasing of VO_x content. Moreover, a higher VO_x content leads to a lower micropore area and micropore volume. The increase in VO_x content also enlarges the pore volume first from 0.27 cm^3/g (V(1.5)/Ti) to 0.31 cm^3/g (V(4.0)/Ti), and then reduces to 0.26 m^3/g (V(8.0)/Ti). Hence, the suitable VO_x content (≤5.74% (in weight) in this study, Table 1) can promote the formation of new porous structures, resulting in an increase in the surface area, mesopore area, and pore volume, which would benefit the

Table 2 The structural properties of the series catalysts

BET parameters	Surface area (SA) (m^2/g)	Mesopore area (MeA) (m^2/g)	Ratio of MeA to SA /	Micropore area (m^2/g)	Pore volume (cm^3/g)	Micropore volume (cm^3/g)	Average pore diameter (nm)
V(1.5)/Ti	49.7	29.7	0.60	20.0	0.27	0.0100	21.8
V(2.5)/Ti	52.2	35.2	0.68	17.0	0.28	0.0085	21.4
V(4.0)/Ti	55.7	44.8	0.80	10.9	0.31	0.0054	21.9
V(5.5)/Ti	58.9	47.0	0.80	11.9	0.28	0.0059	19.0
V(8.0)/Ti	31.5	26.4	0.84	5.1	0.26	0.0025	32.6
V–Ce/Ti	61.5	50.9	0.83	10.6	0.31	0.0052	19.9
V–W/Ti	67.8	60.4	0.89	7.5	0.29	0.0036	17.3
V–Ce–W/Ti	62.0	55.4	0.89	6.6	0.26	0.0032	16.9
TiO_2	90.2	81.1	0.90	9.1	0.39	0.0043	17.1

promotion of the catalytic activity. However, the excessive content of VO_x (8.07% (in weight) in this study, Table 1) can also lead to pore collapse, resulting in a distinct decrease in BET parameters, which could also significantly impair the catalytic activity. Finally, the optimal VO_x content is 4.06% (in weight) in this study, which will be selected for further improvement by introducing CeO_x and WO_x.

Based on V(4.0)/Ti, the addition of CeO_x increases the surface area (61.5 m^2/g) and mesopore area (50.9 m^2/g), while other BET parameters show less change. In comparison, the addition of WO_x increases the surface area (67.8 m^2/g) and mesopore area (60.4 m^2/g) and decreases the micropore area (7.5 m^2/g), as well as the total pore volume (0.29 cm^3/g), micropore volume (0.0036 cm^3/g), and average pore diameter (17.3 nm). These enhancements can provide more reaction interfaces and promote the physisorption of 1,2-DCB over catalysts [15]. Thus, the V–W/Ti might show higher catalytic activity for decomposing 1,2-DCB in this study. The synergistic modification of CeO_x and WO_x also increases the surface area (62.0 m^2/g) and mesopore area (55.4 m^2/g) and decreases the micropore area (6.6 m^2/g), pore volume (0.26 cm^3/g), micropore volume (0.0032 cm^3/g), and average pore diameter (16.9 nm). From other perspectives, the introduction of WO_x promotes the surface area and mesopore area of V–Ce/Ti, while the modification of CeO_x on V–W/Ti decreases them instead as well as other BET parameters. The CeO_x might enhance the catalytic activity of V–W/Ti by other routes, e.g., enlarging the oxygen storage/release capacity and/or speeding up the redox cycle of VO_x, WO_x, and reactive oxygen species [7, 15]. In general, the surface area of V–Ce–W/Ti is better than many commercial catalysts and powdered catalysts prepared in the lab [9, 24–26], which could ensure its high catalytic activities.

Redox properties

As known, it has two essential reaction steps for the catalytic oxidation of chloroaromatic organics over VO_x/TiO_2 catalysts: (1) the nucleophilic adsorption and substitution of the chlorine in the aromatic ring and (2) the subsequent cracking/oxidation of the remaining aromatic ring and intermediates to final products (CO_2, CO, HCl, and H_2O) [3–5, 15]. After surface adsorption of chloroaromatic organics, the subsequent substitution of chlorine, cracking of the aromatic ring, and oxidation of the remaining aromatic ring and intermediates are closely related to the redox cycle of active components (VO_x, CeO_x, and WO_x) and reactive oxygen species.

Figure 2 illustrates the XPS spectra of the V 2p, O 1s, Ce 3d, and W 4f, respectively. The VO_x is the major active component of the catalysts in this study, and its distribution of valence states (V^{5+}, V^{4+}, and V^{3+}) can be closely related to the catalytic activity [3]. The V 2p spectra in Fig. 2a demonstrate that V species exhibit multiple oxidation states. The peaks at binding energies of 517.5 eV (or 524.7 eV), 516.0 eV (or 523.4 eV), and 515.1 eV (or 522.5 eV) correspond to V^{5+}, V^{4+}, and V^{3+}, respectively [27, 28]. By increasing the VO_x content, the signal intensity of V 2p first increases and then decreases, and the highest signal intensity is observed in V(4.0)/Ti. This indicates that the surface concentration of V element achieves the highest in V(4.0)/Ti and excessive VO_x content would not benefit the surface distribution of V species. The catalytic activity of the VO_x/TiO_2 series will also be positively related to the surface concentration of VO_x species. In addition to the intensity change, all peaks assigned to V species are first shifted to higher binding energies and then decrease with increasing VO_x content, and the peaks corresponding to the highest binding energy are also observed in V(4.0)/Ti. This could be ascribed to the increased VO_x content and the optimal chemical environment for V atoms in the VO_x

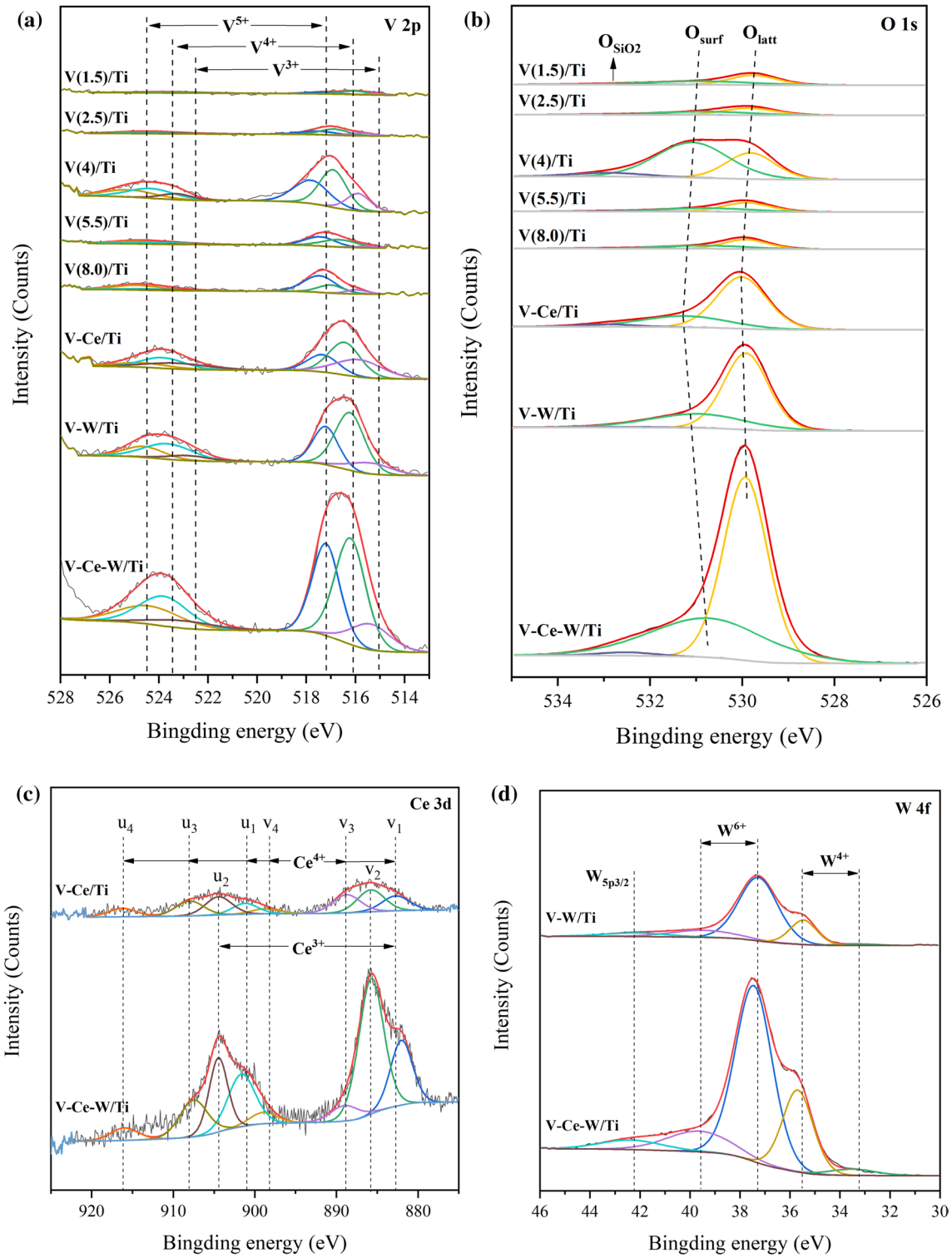

Fig. 2 XPS (X-ray photoelectron spectroscopy) analyses of (**a**) V 2p, (**b**) O 1S, (**c**) Ce 3d, and (**d**) W 4f for series catalysts

species. As a result, the proportions of V^{5+}, V^{4+}, and V^{3+} are significantly changed (Table 3). The V^{5+} proportion is gradually enlarged by increasing the VO_x content, which could enhance the associated catalytic oxidation ability (Table 3). Based on the V(4.0)/Ti, the modification of CeO_x and WO_x further enhances the signal intensity of VO_x species, and the peaks assigned to V species are shifted to lower binding energies (Fig. 2a). On the one hand, the addition

Table 3 XPS spectra of the catalysts (%)

Element valence	V			Ce		W		O		
	V^{5+}	V^{4+}	V^{3+}	Ce^{4+}	Ce^{3+}	W^{6+}	W^{4+}	O_{surf}	O_{latt}	O_{2att}
V(1.5)/Ti	30.2	55.1	14.8					42.5	52.5	5.0
V(2.5)/Ti	34.4	46.8	18.9					43.6	51.4	5.0
V(4.0)/Ti	36.6	44.9	18.5					62.2	31.0	6.8
V(5.5)/Ti	48.3	45.0	6.7					40.6	54.1	5.3
V(8.0)/Ti	64.1	25.2	10.6					38.2	56.4	5.3
V–Ce/Ti	22.6	43.3	34.1	64.9	35.1			26.7	69.2	4.1
V–W/Ti	30.8	54.5	14.7			75.5	18.5	28.2	70.6	1.2
V–Ce–W/Ti	37.2	47.6	15.3	51.2	48.8	69.9	24.9	35.4	63.1	1.5

of CeO_x and WO_x can increase the surface distribution of VO_x species. On the other hand, the introduction of Ce and W atoms would change the chemical environment of the V atom due to the synergistic interaction of VO_x to CeO_x, WO_x, and TiO_2. Interestingly, the introduction of both CeO_x and WO_x reduces the V^{5+} proportion (from 36.6% to 22.6% and 30.8%) (Table 3), which seems to cause a status of valence unsaturation. Subsequently, the V^{3+} proportion in V–Ce/Ti and V^{4+} proportion in V–W/Ti increase. On the contrary, the synergistic addition of CeO_x and WO_x leads to a slight increase in V^{5+} (37.2%) and a decrease in V^{3+} (15.3%). From other perspectives, the modification of WO_x based on V–Ce/Ti and CeO_x based on V–W/Ti both increase their original V^{5+} proportions.

The O 1s spectra of the series VO_x/TiO_2 catalysts (Fig. 2b) contain three peaks with binding energies at around 529.8 eV and 530.9 eV, corresponding to the surface lattice oxygen (O_{latt}) and surface chemisorbed oxygen (O_{surf}), respectively [27, 28]. Similar as VO_x species (Fig. 2a), the signal intensity of O species first increases and then decreases with the increasing VO_x content, and it achieves the highest level in V(4.0)/Ti (Fig. 2b). Moreover, the modification of CeO_x and/or WO_x further enhances the signal intensity of O species. The peaks assigned to O_{latt}, O_{surf}, and O_{SiO2} shifted to different binding energies, i.e., the increase in VO_x content and addition of CeO_x caused the shifts to higher binding energies, while the opposite shift was caused by the modification of CeO_x and WO_x. Usually, O_{surf} refers to the oxygen-free radicals (e.g., O, O^-, and O^{2-}) that are weakly bonded to surface metal atoms (V, Ce, and W in this study) and are easily supplied to the reaction of oxidation and reduction [15]. Therefore, the proportion of O_{surf} is regarded as an essential indicator of catalytic activity toward the 1,2-DCB catalytic oxidation [6]. Table 3 shows that the increase in VO_x content leads to a similar change in O_{surf} proportions to the signal intensity of O 1s. Interestingly, the modification of CeO_x and/or WO_x based on V(4.0)/Ti reduces the O_{surf} proportion to 26.7%–35.4%, but the modification of WO_x for V–Ce/Ti and CeO_x for V–W/Ti both increase their original O_{surf} proportions. The former could be ascribed to that the introduction of CeO_x and WO_x facilitating more to the O_{latt} and enhancing the oxygen storage capacity. The latter confirms that both CeO_x and WO_x can also benefit the enhancement of O_{surf}.

The Ce 3d spectra (Fig. 2c) can be deconvoluted into eight small peaks corresponding to Ce^{4+} (v_1, v_3, v_4, u_1, u_3, and u_4) and Ce^{3+} (v_2 and u_2), respectively [15, 27]. The addition of WO_x significantly enhances the signal intensity of Ce species. The peaks assigned to Ce^{4+} have a slight shift in their binding energies due to the modification of WO_x, which shows less influence on the peaks assigned to Ce^{3+}. Table 3 reports the introduction of WO_x reduces the Ce^{4+} proportion from 64.9% to 51.2% and increases the Ce^{3+} proportion from 35.1% to 48.8%, indicating that the WO_x species improved the electron transfer of the catalysts to facilitate the formation of reduced CeO_x that could be essential to enhance the formation of superoxide ions (i.e., lead to higher oxygen storage capacity).

The W 4f spectra (Fig. 2d) contain peaks at binding energies of 37.27 eV (or 39.45 eV), 33.29 eV (or 35.47 eV), and 42.14 eV corresponding to W^{6+}, W^{4+}, and W 5p3/2, respectively [27]. The addition of CeO_x distinctly improves the signal intensity of W species. The five peaks are shifted to higher binding energies. Table 3 illustrates that CeO_x reduces the W^{6+} (from 75.5% to 69.9%) and increases the W^{4+} (from 18.5% to 24.9%). In addition to the slight enhancement of the oxygen storage capacity, it also impairs the O_{latt} proportion with lower mobility of oxygen species but improves the O_{surf} proportion with a flexible supplement to the oxidation reaction [29, 30].

Overall, the modification of both CeO_x and WO_x can either enhance the surface content of V species or enlarge the V^{5+} proportion, which could benefit the catalytic oxidation of chloroaromatic organics. Moreover, they can improve the surface content of oxygen species, as well as enrich the surface oxygen-free radicals (e.g., O, O^-, and O^{2-}) and oxygen storage capacity, which can facilitate the catalytic oxidation of 1,2-DCB by providing abundant reactive oxygen species and accelerating the redox cycle of V, Ce, and W.

Evaluation of catalytic activity

To evaluate the catalytic activity of series catalysts, this study focuses on the CE of 1,2-DCB and the CO_2 selectivity of the converted 1,2-DCB, as shown in Fig. 3. The former represents the removal efficiency of 1,2-DCB over series catalysts, and the latter refers to their complete oxidation ability to mineralize the 1,2-DCB into the final products (CO_2, HCl, H_2O), i.e., higher selectivity represents fewer intermediates. Figure 3a illustrates the CE of 1,2-DCB over VO_x/TiO_2. By increasing the proportion of VO_x from 1.50% to 8.07% (in weight), the CE values of 1,2-DCB first increased and then decreased, i.e., a higher content of VO_x is not equal to higher catalytic activity. Among these VO_x/TiO_2 catalysts, V(4.0)/Ti has the highest CE of 1,2-DCB (65.2%–73.3%) in the low-temperature range (150–200 °C), which corresponds to the intensity changes of V and O determined by XPS as well as the changing trend of surface area and mesopore area determined by BET. It is unsurprising that a higher reaction temperature will lead to a faster redox cycle of VO_x, resulting in a higher CE of 1,2-DCB over each catalyst and fewer intermediate residues [3]. Especially for the V(1.5)/Ti and V(2.5)/Ti, the increase in reaction temperature contributes to a greater improvement in the CE, i.e., the CE increases from 1.8% to 56.2% (V(1.5)/Ti) and from 16.2% to 63.7% in the temperature range of 150–200 °C (V(2.5)/Ti). Unlike them, the V(4.0)/Ti and V(5.5)/Ti can achieve high CE (65.2%–74.5%, 61.8%–66.3%, respectively) at relatively

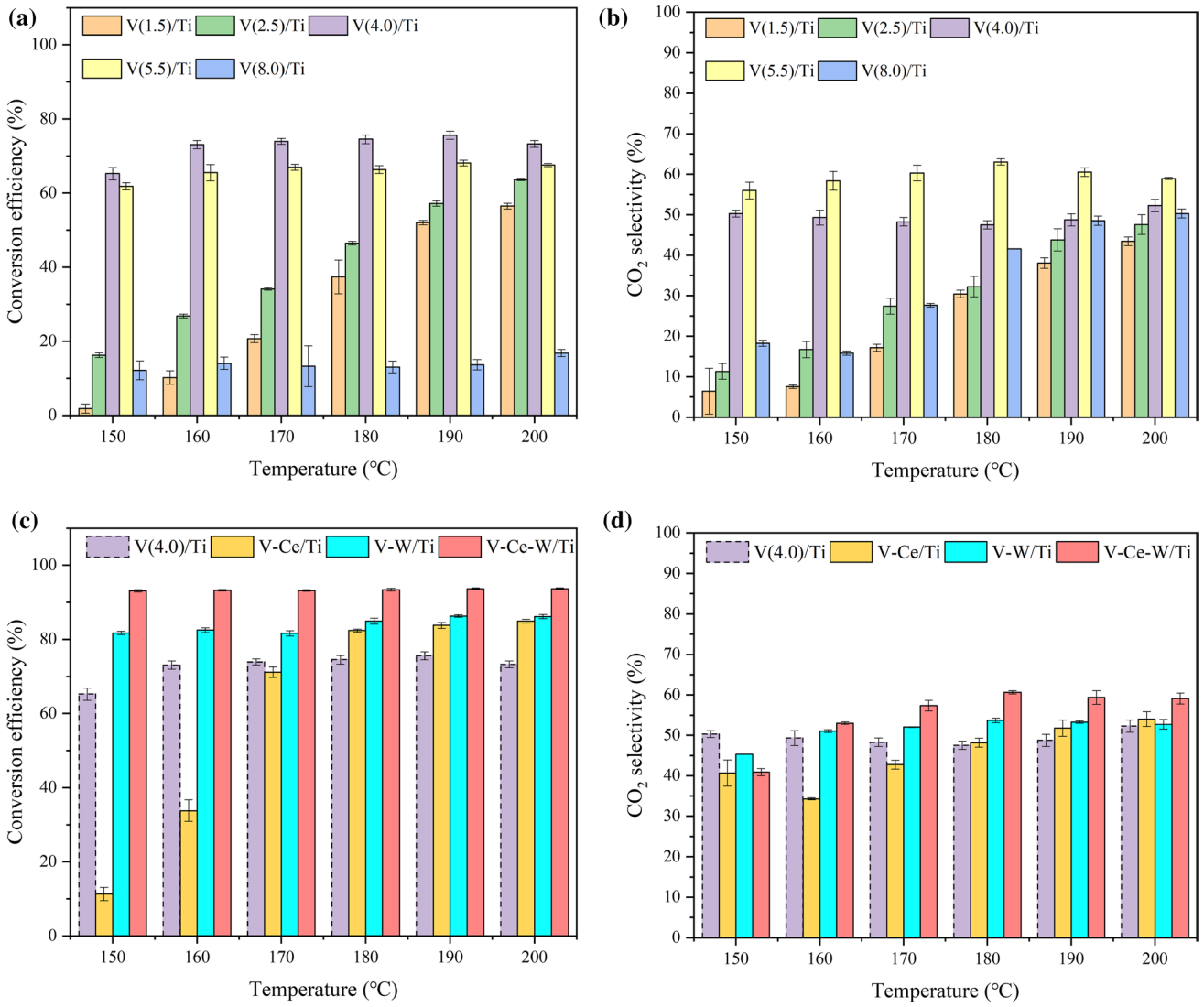

Fig. 3 The CE and CO_2 selectivity of 1,2-DCB of series catalysts. (**a**) conversion efficiency of series VO_x/Ti catalysts; (**b**) CO_2 selectivity of series VO_x/Ti catalysts; (**c**) conversion efficiency of modified VO_x/Ti catalysts; (**d**) CO_2 selectivity of modified VO_x/Ti catalysts. *CE* conversion efficiency

lower reaction temperature (≤180 °C), which could benefit from the higher surface distribution of VO_x species and oxygen storage (especially O_{surf}), as well as their abundant porous structure. For V(8.0)/Ti, the general CE is as low as 12.2%–16.8%, which is even worse than that of V(1.5)/Ti at higher reaction temperatures (≥170 °C). This is ascribed to its poor physisorption first, followed by its weak redox ability. This work also suspects that the residues of the shaping additives will influence the catalytic activity, which is not supported by the XRF and XPS results.

To gain insight into the oxidation reaction, the CO_2 selectivity is essential evidence for revealing the complete oxidation ability of 1,2-DCB. As shown in Fig. 3b, a higher reaction temperature also leads to higher CO_2 selectivity, which is evident not only on the V(1.5)/Ti and V(2.5)/Ti but also on the V(8.0)/Ti. Although the CE of 1,2-DCB over V(8.0)/Ti is very low (Fig. 3a), its CO_2 selectivity shows a high level (15.8%–50.3%) (Fig. 3b). From the perspective of CO_2 selectivity, the disadvantages of the above three catalysts are their poor performance at lower temperatures (≤180 °C). On the contrary, both V(4.0)/Ti and V(5.5)/Ti show high complete oxidation ability in the same temperature window. Besides, the V(5.5)/Ti shows the highest CO_2 selectivity (56.0%–63.0%) rather than V(4.0)/Ti (47.5%–52.3%), which is more correlated with their V^{5+} proportions. Based on the BET parameters and XPS analysis, especially at higher reaction temperatures (190 °C and 200 °C), the CE of 1,2-DCB is positively correlated with the surface area, mesopore area, signal intensity of V and O species, as well as the O_{surf} proportion, while the CO_2 selectivity is more consistent with the proportion of V^{5+} and surface content of VO_x species.

Based on the above analysis, the subsequent improvement is based on the optimal formulation of V(4.0)/Ti. Figure 3c illustrates the CE of 1,2-DCB over catalysts modified by CeO_x and WO_x. The CE of 1,2-DCB over V–Ce/Ti is distinctly reduced (11.3%–71.2%) at lower temperatures (≤170 °C) but is improved (82.4%–84.9%) at higher temperatures (>170 ℃). The CO_2 selectivity (complete catalytic oxidation ability) shows similar phenomenon. As a comparison, V–W/Ti increases the CE to 81.6%–86.3%, as well as the CO_2 selectivity (45.3%–53.7%), which are all higher than those of V(4.0)/Ti except for the CO_2 selectivity (45.3%) at 150 °C. However, this difference is eliminated by increasing the reaction temperature, i.e., the CE over V–Ce/Ti and V–W/Ti is very close, and the CO_2 selectivity of V–Ce/Ti is even higher than that of V–W/Ti. The former could be ascribed to the better improvement of WO_x than CeO_x, including higher surface area, mesopore area, the proportion of V^{5+} and O_{surf}, and the V^{3+} proportion in V–Ce/Ti is relatively high (34.1%), which causes the V species to exist in a relative reduction status and impaires the catalytic activity at lower reaction temperatures (150–160 °C). The latter could be attributed to the enhancement of higher temperature on the redox cycle of VO_x, CeO_x, and reactive oxygen species, leading to high catalytic activity at higher reaction temperatures (180–200 °C). However, both the CeO_x and WO_x improve the CO_2 selectivity less, i.e., the complete oxidation ability is less enhanced, which should be further improved to reduce intermediate generation.

Due to the synergistic modification of CeO_x and WO_x, the V–Ce–W/Ti achieves the highest CE of 93.1%–93.6%, and the CO_2 selectivity is further increased to 40.9%–60.7%. All of these values are higher than those of V(4.0)/Ti, V–Ce/Ti, and V–W/Ti except for the CO_2 selectivity at 150 °C. From other perspectives, the addition of WO_x to V–Ce/Ti or the addition of CeO_x to V–W/Ti can both improve the catalytic activity of original catalysts. That is, the modification of WO_x could overcome the low catalytic activity of V–Ce/Ti at 150–160 ℃ and increase the general catalytic oxidation ability. The introduction of CeO_x can further improve the V–W/Ti in these two aspects. Note that the CO_2 selectivity of V(5.5)/Ti (Fig. 3b) is generally higher than that of V–Ce–W/Ti (Fig. 3d), indicating that a higher VO_x content could benefit the chemisorption and nucleophilic substitution of 1,2-DCB by V=O species, as well as the subsequent cracking of the ring structure and oxidation to form the final products [4]. However, the enhanced chemisorption and nucleophilic substitution of 1,2-DCB could also lead to the harder release of the intermediates and cause the low CE of V(8.0)/Ti (Fig. 3a). Therefore, these results further confirm that CeO_x and WO_x mainly promote catalytic activity by other routes. On one hand, the CeO_x and WO_x can increase the catalytic activity by improving the proportion of V^{5+} and O_{surf}. On the other hand, the existence of CeO_x and WO_x enriches the supply source of reactive oxygen species and their storage capacity, and they can also accelerate the redox cycle of VO_x, CeO_x, WO_x, and reactive oxygen species.

Based on this study, the newly developed V–Ce–W/Ti catalyst shows high catalytic activity in eliminating 1,2-DCB at low temperature, which could be a good choice for industrial applications due to its lower energy consumption and operating cost. However, its CO_2 selectivity could be further improved, which will facilitate less emission of organic intermediates. In addition, catalytic activity evaluation of PCDD/Fs, NO_x, the resistance to SO_2, HCl, heavy metals, etc., and the pilot test with actual flue gas will be further conducted in the next step. In addition, further characterization of these eight honeycomb-type catalysts is still necessary to be conducted, which will reveal the in-depth modification mechanism of CeO_x and WO_x.

Conclusions

This study develops a series of honeycomb-type VO_x/TiO_2 catalysts and finally obtains a new low-temperature catalyst for eliminating chloroaromatic organics in the MSWI flue gas. Based on the CE of 1,2-DCB and CO_2 selectivity, the VO_x content of 4.06% (in weight) in V(4.0)/Ti is confirmed as the optimal formulation. By modifying CeO_x and WO_x, V–Ce–W/Ti achieves the highest CE (93.1%–93.6%) and CO_2 selectivity (40.9%–60.7%) at 150–200 °C. CeO_x and WO_x can improve the catalytic activity by enhancing the surface content of V and O, increasing the proportion of V^{5+} and O_{surf}, enlarging the supply source of reactive oxygen species and their storage capacity, and accelerating the redox cycle of VO_x, CeO_x, WO_x, and reactive oxygen species. These results are meaningful for developing new low-temperature SCR catalysts with high catalytic activity in eliminating chloroaromatic organics in the future.

Acknowledgements This study is supported by the National Key Research and Development Program of China (No. 2020YFC1910100).

Declarations

Conflict of interest On behalf of all authors, the corresponding author states that there is no conflict of interest.

References

1. NBSC (National Bureau of Statistics). 2021. *China Statistical Yearbook*. Beijing, China: China Statistical Press.
2. Peng, Y.Q., Lu, S.Y., and Li, X.D. 2020. Formation, measurement, and control of dioxins from the incineration of municipal solid wastes: Recent advances and perspectives. *Energy & Fuels* 34(11): 13247–13267.
3. Du, C.C., Lu, S.Y., Wang, Q.L., et al. 2018. A review on catalytic oxidation of chloroaromatics from flue gas. *Chemical Engineering Journal* 334: 519–544.
4. Wang, J., Wang, X., Liu, X.L., et al. 2015. Kinetics and mechanism study on catalytic oxidation of chlorobenzene over V_2O_5/TiO_2 catalysts. *Journal of Molecular Catalysis A: Chemical* 402: 1–9.
5. Wang, J., Wang, X., Liu, X.L., et al. 2015. Catalytic oxidation of chlorinated benzenes over V_2O_5/TiO_2 catalysts: The effects of chlorine substituents. *Catalysis Today* 241: 92–99.
6. Wang, D., Chen, J.J., Peng, Y., et al. 2018. Dechlorination of chlorobenzene on vanadium-based catalysts for low-temperature SCR. *Chemical Communications* 54(16): 2032–2035.
7. Wang, Q., Hung, P.C., Lu, S., et al. 2016. Catalytic decomposition of gaseous PCDD/Fs over V_2O_5/TiO_2-CNTs catalyst: Effect of NO and NH_3 addition. *Chemosphere* 159: 132–137.
8. Yu, M.F., Li, X.D., Ren, Y., et al. 2016. Low temperature oxidation of PCDD/Fs by TiO_2-based V_2O_5/WO_3 catalyst. *Environmental Progress & Sustainable Energy* 35(5): 1265–1273.
9. Yu, M.F., Li, W.W., Li, X.D., et al. 2016. Development of new transition metal oxide catalysts for the destruction of PCDD/Fs. *Chemosphere* 156: 383–391.
10. Chen, C.M., Cao, Y., Liu, S.T., et al. 2018. Review on the latest developments in modified vanadium-titanium-based SCR catalysts. *Chinese Journal of Catalysis* 39(8): 1347–1365.
11. Han, L.P., Cai, S.X., Gao, M., et al. 2019. Selective catalytic reduction of NO_x with NH_3 by using novel catalysts: State of the art and future prospects. *Chemical Reviews* 119(19): 10916–10976.
12. Goemans, M., Clarysse, P., Joannès, J., et al. 2003. Catalytic NO*x* reduction with simultaneous dioxin and furan oxidation. *Chemosphere* 50(4): 489–497.
13. Lin, X.Q., Ma, Y.F., Chen, Z.L., et al. 2020. Effect of different air pollution control devices on the gas/solid-phase distribution of PCDD/F in a full-scale municipal solid waste incinerator. *Environmental Pollution* 265(Part B): 114888.
14. Liu, X.L., Wang, J., Wang, X., et al. 2015. Simultaneous removal of PCDD/Fs and NO_x from the flue gas of a municipal solid waste incinerator with a pilot plant. *Chemosphere* 133: 90–96.
15. Wang, Q., Huang, X., Feng, Y., et al. 2021. Interaction mechanism study on simultaneous removal of 1,2-dichlorobenzene and NO over MnO_x–CeO_2/TiO_2 catalysts at low temperatures. *Industrial & Engineering Chemistry Research* 60(13): 4820–4830.
16. Huang, H. 2018. *Preparation of honeycomb* V_2O_5-WO_3/TiO_2 *catalyst and its catalytic degradation experiment[D]*. Zhejiang University.
17. Chung, K., Jiang, Z., Gill, B., et al. 2002. Oxidative decomposition of o-dichlorobenzene over V_2O_5/TiO_2 catalyst washcoated onto wire-mesh honeycombs. *Applied Catalysis A: General* 237(1–2): 81–89.
18. Weng, X.L., Sun, P.F., Long, Y., et al. 2017. Catalytic oxidation of chlorobenzene over $Mn_xCe_{1-x}O_2$/HZSM-5 catalysts: A study with practical implications. *Environmental Science & Technology* 51(14): 8057–8066.
19. Standardization Administration of the People's Republic of China. 2015. Analytical method of chemical composition for flue gas $DeNO_x$ catalysts. GB/T 31590-2015. Beijing, China: China Quality and Standards Publishing & Media Co., Ltd., pp. 8.
20. Finocchio, E., Busca, G., and Notaro, M. 2006. A review of catalytic processes for the destruction of PCDD and PCDF from waste gases. *Applied Catalysis B: Environmental* 62(1–2): 12–20.
21. Lin, F., Wang, Q.L., Zhang, J.C., et al. 2019. Mechanism and kinetics study on low-temperature NH_3-SCR over manganese-cerium composite oxide catalysts. *Industrial & Engineering Chemistry Research* 58(51): 22763–22770.
22. Zhang, S.L. and Zhong, Q. 2013. Promotional effect of WO_3 on O_2^- over V_2O_5/TiO_2 catalyst for selective catalytic reduction of NO with NH_3. *Journal of Molecular Catalysis A: Chemical* 373: 108–113.
23. Yu, M.F., Lin, X.Q., Li, X.D., et al. 2016. Catalytic destruction of PCDD/Fs over vanadium oxide-based catalysts. *Environmental Science & Pollution Research International* 23: 16249–16258.
24. Debecker, D.P., Delaigle, R., Hung, P.C., et al. 2011. Evaluation of PCDD/F oxidation catalysts: Confronting studies on model molecules with tests on PCDD/F-containing gas stream. *Chemosphere* 82(9): 1337–1342.
25. Gallastegi-Villa, M., Aranzabal, A., González-Marcos, M.P., et al. 2020. Effect of vanadia loading on acidic and redox properties of VO_x/TiO_2 for the simultaneous abatement of PCDD/Fs and NO_x. *Journal of Industrial and Engineering Chemistry* 81: 440–450.
26. Zhan, M.X., Ji, L.J., Ma, Y.F., et al. 2018. The impact of hydrochloric acid on the catalytic destruction behavior of 1,2-dichlorbenzene and PCDD/Fs in the presence of VWTi catalysts. *Waste Management* 78: 249–257.
27. Moulder, J.F., Stickle, W.F., Sobol, P.E., et al. 1992. Handbook of X-ray Photoelectron Spectroscopy. Eden Prairie, MN, USA: Perkin-Elmer Corporation.
28. Weng, X.L., Xue, Y., Chen, J.K., et al. 2020. Elimination of chloroaromatic congeners on a commercial V_2O_5-WO_3/TiO_2 catalyst: The effect of heavy metal Pb. *Journal of Hazardous Materials* 387: 121705.

29. Liu, Z.M., Zhang, S.X., Li, J.H., et al. 2014. Novel V_2O_5–CeO_2/TiO_2 catalyst with low vanadium loading for the selective catalytic reduction of NO_x by NH_3. *Applied Catalysis B: Environmental* 158–159: 11–19.
30. Wang, Q.L., Zhou, J.J., Zhang, J.C., et al. 2020. Effect of ceria doping on catalytic activity and SO_2 resistance of MnO_x /TiO_2 catalysts for selective catalytic reduction of NO with NH_3 at low temperature. *Aerosol and Air Quality Research* 20(3): 477–488.